

Natural abundance ^{15}N CP/MAS n.m.r. of solid polyamides: a technique sensitive to composition and conformation in the solid state

Douglas G. Powell, Allison M. Sikes* and Lon J. Mathias†

Department of Polymer Science, University of Southern Mississippi, Hattiesburg, MS 39406-0076, USA

(Received 7 August 1989; revised 13 September 1990; accepted 13 September 1990)

High resolution solid state ^{15}N nuclear magnetic resonance (n.m.r.) of several AB and AA-BB polyamides were obtained at the nitrogen natural abundance level. Resonances at 84 and 89 ppm (relative to solid glycine) clearly correspond to α and γ crystal forms, respectively. In addition, a broad intermediate peak (84–89 ppm) is assigned to rigid non-crystalline amorphous and interphase regions in these semicrystalline polymer samples. Confirmation of these assignments involved analysis of ^{15}N -enriched samples of nylon 6 and nylon 11. In addition, a high-temperature δ form for nylon 11 (labelled sample) was found to give a peak at 86.6 ppm while a metastable δ' form obtained by quenching from the melt gave an identical chemical shift value. Cross-polarization/magic angle spinning (CP/MAS) spectra coupled with spin-lattice relaxation measurements of the labelled samples further confirmed the identity of peaks for amorphous regions and the various individual crystal forms. Commercial amorphous nylons were also examined by ^{15}N CP/MAS and found to give a broad envelope of resonances (80–90 ppm) indicative of random conformations around the amide groups. The origin of the chemical shift differences is rationalized in terms of polymethylene chain conformation relative to the plane of the amide group. Semi-empirical molecular orbital calculations of model amides show electron density variations which correlate with the shielding and deshielding of the nitrogen atom consistent with this interpretation. Based on these results, ^{15}N solid state n.m.r. is found to be a sensitive technique for examining local conformations in solid polyamides even with natural abundance ^{15}N samples.

(Keywords: CP/MAS n.m.r.; polyamides; solid state)

INTRODUCTION

Analysis of the morphology and composition of solid polymers is inherently more difficult than that of small molecule crystals and glasses. Thermal analysis and dynamic mechanical analysis have been used to evaluate molecular mobility, relaxation processes and thermal transitions in solid polymers¹. Spectroscopic techniques have included mainly X-ray diffraction and infra-red for determining the type and degree of crystallinity, and order in semicrystalline polymers such as polyamides^{2,3}. Recently, solid state nuclear magnetic resonance (n.m.r.) has been developing as a sensitive tool for measuring motion and order using both high-speed spinning and non-spinning methods, and focusing mainly on ^{13}C cross-polarization/magic angle spinning (CP/MAS), ^2H wide-line and ^1H multi-pulse techniques^{4–6}.

We have been attempting to develop a two-pronged approach to new polymers and polymeric materials. On the one hand, we are employing new synthetic concepts combining polymer formation with processing to generate the desired product composition in a single step. For example, we have made several high performance polymers and molecular composites with controlled, *in situ* generation of the final structures^{7–10}. On the other

hand, we are exploring newly available spectral and physical analytical methods which allow molecular characterization of such materials. These methods give information relating as-obtained or end-use molecular composition and microscopic properties to macroscopic behaviour. For the latter case, we have been examining the use of natural abundance ^{15}N CP/MAS n.m.r. for evaluating composition and morphology of a variety of aramids, polyamides, polyimides, urethanes and epoxies. We have already reported¹¹ our initial results on the characteristic peaks seen in ^{15}N CP/MAS spectra for the two main crystalline forms of nylon 6 and on the multiple peaks seen in longer alkyl polyamides corresponding to the two crystalline forms and the amorphous components¹².

Subsequently, we prepared and characterized ^{15}N -labelled nylon 6 and nylon 11 in order to confirm peak assignments, especially for peaks associated with amorphous domains^{13–15}. The isotopically enriched samples confirmed the presence of both crystalline forms and the amorphous regions of the polymers. In addition, the first ^{15}N relaxation measurements of a polyamide were obtained on the labelled samples, and the results correlated well with the semicrystalline morphology of the polyamides^{14,15}. After our initial results were reported, Hatfield and co-workers confirmed our ^{15}N chemical shift observations¹⁶ on nylon 6.

We have now characterized a range of aliphatic

* Present address: Coatings Section, Naval Research Laboratory, Washington DC 20375, USA

† To whom correspondence should be addressed

polyamides and report here the characteristic peaks for amide nitrogens in the two main crystalline forms (α and γ forms) and the amorphous regions. In addition, we discuss the origin of polyamide chemical shifts in terms of conformationally dependent interaction between the plane of the amide group and the attached methylene groups as demonstrated by semi-empirical molecular orbital (MO) calculations.

EXPERIMENTAL

Nylon 6 and nylon 6-6 polyamides were obtained from Aldrich Chemical Company (Milwaukee, WI). Amorphous nylons Zytel 330, APC-110 and APC-121 were obtained from DuPont Chemical Co. (Parkersburg, WV). Nylons 11, 12, 6-9, 6-10, 6-12 and 6-T were obtained from Scientific Polymer Products (Ontario, NY). Nylon 13-13 was obtained from Professor R. S. Porter, University of Massachusetts. Nylon 3 [poly(β -alanine)] was prepared by the anionic polymerization of acrylamide. Nylon 4 was obtained from Chevron Research Company (Richmond, CA). Glycine peptide oligomers and Gly- β -Ala were obtained from Sigma Chemical Company (St Louis, MO). The peptides were obtained as crystalline powders and used as received. Commercial polyamides were received as small pellets 1–2 mm in diameter. ¹⁵N-enriched nylon 6 and nylon 11 were prepared in our laboratory. The nylon 11 characterization work was carried out in collaboration with J. P. Autran and Professor R. S. Porter of the University of Massachusetts¹⁵.

The polyamides generally were melt pressed between layers of aluminum foil on a heated hydraulic press at 0.5–0.6 MPa to give films of uniform thickness of \sim 0.1 mm. The press temperature was adjusted to 20°C or so above the observed melting temperature of each sample. Cooling rates of the molten samples were adjusted to give the desired crystal forms¹⁶. This treatment gave samples with maximum estimated crystallinity of 40–45%. Some samples were annealed further under nitrogen or vacuum after film formation. The polyamides synthesized were examined as precipitated powders or pressed films. The presence of α , γ and δ crystal forms was confirmed using infra-red (i.r., Nicolet 5DX FT-IR) and wide-angle X-ray (Phillips PW 1720 X-ray unit using a wavelength of 0.154 nm) methods previously described^{2,3}.

Theoretical models were constructed using PCMODEL, a molecular mechanics package suitable for IBM-PC compatible computers (Serena Software, Bloomington, IN). The geometries of the model amides were first optimized using PCMODEL and the data prepared for MO calculations. Semi-empirical MO calculations were performed using AMPAC, a general purpose modelling package operating on a VAX 11/780 computer and utilizing the AM1 basis set¹⁷.

Solid state ¹⁵N CP/MAS n.m.r. spectra were obtained on a Bruker MSL 200 spectrometer equipped with a Bruker MAS solids probe. A standard CP pulse sequence was used with a ¹H 90° pulse of 5 μ s and a contact pulse of 1–5 ms. A recycle delay of 3 s (\sim 3 T_{1H}) was inserted between successive scans. From 1000 to 10 000 scans were collected for each sample. The spectral width was 25 kHz. The acquisition time was adjusted to give a digital resolution of 3.05 Hz per point. Lorentzian line

broadening of 5–20 Hz was performed on the free induction decay before Fourier transformation. The MAS rotor speeds were 3–5 kHz. Unless otherwise indicated, all measurements were made at 300 K. Chemical shifts are reported relative to solid glycine (at 0 ppm) as an external reference. Literature ¹⁵N chemical shifts reported in Table 1 are converted to the glycine scale for comparison (nitromethane = 347 ppm and *NH₄NO₃ = –11.3 ppm on the glycine scale).

RESULTS AND DISCUSSION

Aliphatic polyamides

Several reports have appeared on ¹⁵N CP/MAS of synthetic and natural polypeptides showing strong dependence of chemical shift on composition, conformation and the presence of β -alkyl substituents^{18–20}. Nylon 6 possesses both an all-coplanar and all-*trans* α form crystalline modification (Figure 1a), and a γ form (Figure 1b) in which the amide groups are rotated \sim 60° out of the plane of the polymethylene zig-zag^{21,22}. We earlier described the ¹⁵N CP/MAS results for nylon 6 and several block and random copolymers containing nylon 6 units¹¹. Peaks were reported only for the α and γ forms of this polymer (confirmed by i.r. and X-ray data) at 84.1 and 89.1 ppm since these were by far the most intense peaks observed. A downfield shift of 5 ppm was observed on going from the more thermodynamically stable α form to the γ form possessing the out-of-plane amide group.

Subsequent analysis was carried out on several nylons whose crystal structures had been previously determined^{23–29}. We were surprised at the complexity of the spectra obtained and postulated that broad peaks were being observed for the various amide conformations in the ‘amorphous’ regions¹². We have now completed a survey of additionally available polyamides containing alkyl and alkyl-aryl groups in the backbone. Polyamide ¹⁵N chemical shifts are given in Tables 1 and 2 along with predominant crystal form(s) reported by others^{23–29}. We are now able to assign all peaks in the spectra obtained. We believe these results, especially the natural abundance data, will stimulate additional study of the use of ¹⁵N CP/MAS n.m.r. in the characterization of such polymers. In general, this method provides a useful approach to determining the molecular environment of amide groups in polyamides.

Figures 2–4 give representative spectra. The lowest trace (A) in Figure 2 was observed for a nylon 6-10 sample that had been melt pressed into a clear thin film and annealed to promote formation of the thermodynamically stable (for this polymer) α crystalline form. The peak at 83.8 δ is relatively sharp with a peak width at half-height of only 3.2 ppm. Trace B is the spectrum of the similarly produced γ form of nylon 12. The peak is located at 88.7 δ and has a peak width of 4.1 ppm. These two spectra represent some of the cleanest n.m.r. examples we have seen to date of these two crystal forms at the ¹⁵N natural abundance level.

Trace C in Figure 2 was obtained on a nylon 6-10 sample which had been melt pressed and rapidly quenched to room temperature. It shows a broad peak from 83 to 90 ppm which encompasses the residual α form (which was seen at 84 ppm above) and possibly a small amount of γ form (which should be at 89 ppm). In addition, the broad peak contribution between these

Table 1 Characteristic ¹⁵N n.m.r. peaks for aliphatic A-B and AA-BB polyamides

Sample	Treatment	Predominant crystal form	Chemical shifts ^a		
Nylon 2 (Gly)	-	α helix	78.5 ^b		
Nylon 2 (Gly)	-	β sheet	74.0 ^b		
Gly-Gly	-	-	83.9		
Gly- β -Ala	-	-	83.7		
Triglycine	-	-	77.6 75.5		
Tetraglycine	-	-	76.9 71.6		
Pentaglycine	-	-	77.5 76.1 71.4		
Hexaglycine	-	-	76.7 74.8 71.5		
Poly(Ala)	-	α helix	89.1 ^b		
Poly(Ala)	-	β sheet	97.9 ^b		
Nylon 3 (β -Ala)	-	α^c	88.1		
Nylon 4	-	α^d	85.2		
Nylon 6	Slow/250 K	α^e	84.2		
Nylon 6	Quench/250 K	-	89.0 84.3		
Nylon 6	KI/I ₂ treat.	γ^e	84-89(broad)		
Nylon 7	Slow/250 K	α^f	86-88 ^g 85.4		
Nylon 11	Slow/250 K	α^f	84.2		
Nylon 11 ^h	Quench/250 K	δ^i	86.6(broad)		
Nylon 11 ^h	Ppt/CF ₃ CO ₂ H	γ	88.8		
Nylon 11 ^h	CP/MAS at 115 K	δ	86.6		
Nylon 12	Slow/250 K	γ^i	88.9		
Nylon 12	Quench/250 K	-	88.3 86.5 85.6 ^g		
Nylon 6-6	Slow/250 K	α^f	87.4 ^g 84.0		
Nylon 6-8	Slow/250 K	α^f	86-88 ^g 85.6		
Nylon 6-9	Slow/250 K	α^f	86-90		
Nylon 6-10	Slow/250 K	α^f	88.6 ^g 85.8 83.8		
Nylon 6-10	Quench/250 K	-	87.5 85.5		
Nylon 6-12	Slow/250 K	-	83.9		
Nylon 6-12	Quenched	-	85-88(broad) ^g 83.7		
Nylon 13-13	Annealed	-	89.2 84-89(broad) ^g		
Nylon 13-13	Quenched	-	84-89(broad)		

Peaks in italics are the most intense in each spectrum and crystal forms listed were reported by others in the references given

^aIn ppm downfield from glycine ($\delta = 0$ ppm)

^bData taken from ref. 19

^cFrom ref. 25

^dFrom ref. 26

^eFrom ref. 27

^fFrom ref. 28

^gShoulder on main peaks

^h99% ¹⁵N-labelled sample

ⁱFrom ref. 29

two extremes is assigned to the amorphous regions as observed for nylons 6¹⁴ and 11¹⁵. Trace D (quenched nylon 11) shows a similar broad peak which encompasses the stable α form at ~ 84 ppm (as seen for the labelled material) along with a broad shoulder for the amorphous component at 84-89 ppm (confirmed in the spectra of various samples of ¹⁵N-labelled nylon 11¹⁵).

Figure 3 gives spectra for three additional annealed samples reported to prefer the α crystal form²³⁻²⁹. Trace A is of nylon 7 and trace B of nylon 6-8, both of which are reported to prefer the α crystalline form. A sharp peak at 85.4 is seen for nylon 7 overlapped by a broad shoulder corresponding to the amorphous regions at 85-89 ppm. This broad amorphous peak is more intense for the nylon 6-8 sample indicating a reduced α form

content and greater amorphous component. Trace C shows even more amorphous content as indicated by the more intense envelope from 85 to 90 ppm. We believe the shoulder at 85.4 ppm corresponds to the relatively low α content which is reported to be the thermodynamically preferred crystal form²³⁻²⁹.

Figure 4 illustrates the effect of annealing on the crystal content for nylon 13-13. Trace A is of the as-obtained material and shows only the broad amorphous peak between 85 ppm and 89 ppm. On annealing for several hours, this sample developed a sharp peak corresponding to the γ form at 89.2. While these two spectra each required 18 h for acquisition, the analysis time is not significantly greater than that needed for alternative methods. More importantly, the n.m.r. data do not

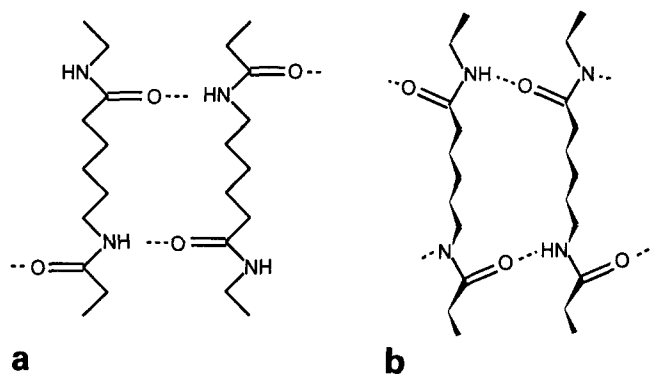


Figure 1 Chain configurations of (a) α and (b) γ nylon 6

Table 2 Characteristic ¹⁵N n.m.r. peaks for amorphous polyamides and alkyl-aryl copolyamides

Polymer	Treatment/history	Chemical shifts ^a	
A-N6/PBA ^b	Ppt reaction mix.	<i>101.6</i>	<i>80.9</i>
Nylon 6-T ^c	Cool from 350 K	<i>86.3</i>	
Zytel 330 ^d	Cool from 350 K	77-88(broad)	
APC-121 ^d	Slow cool from 350 K	77-90(broad)	
APC-110 ^e	Commercial pellets	89-100(broad)	

Peaks in italics are the most intense in each spectrum

^aIn ppm downfield from glycine ($\delta = 0$ ppm)

^bAlternating copolymer of nylon 6 (N6) and *p*-aminobenzoic acid (PBA)

^cPoly(hexamethyleneterephthalamide) obtained from Scientific Polymer Products Inc.

^dDonated samples from E. I. duPont de Nemours Co. Inc. (Parkersburg, WV)

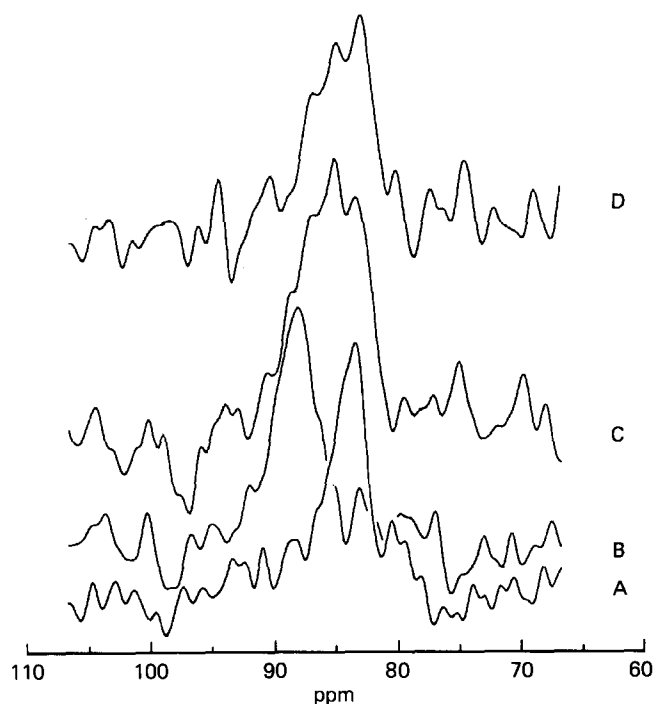


Figure 2 ¹⁵N CP/MAS n.m.r. spectra of commercial nylons: (A) nylon 6-10 annealed α crystal form; (B) nylon 12 γ crystal form; (C) nylon 6-10 sample quenched from the melt; (D) nylon 11 containing predominantly α crystal form

depend as much on size and perfection of the crystalline regions as X-ray analysis, and gives immediate qualitative identification of the type of crystallinity present. Perhaps more important, the n.m.r. data in trace A clearly

confirm the absence of a large amount (perhaps <10%) of either α and γ crystalline domains.

Polymers are not single crystals and correlations with single crystal models may be inappropriate³⁰. The broad peaks and shoulders on sharp peaks arise from rigid interphase or transition zones between α and γ regions as well as amorphous regions as shown schematically in Figure 5. In an elegant discussion on crystal forms of nylon 6, Parker and Lindenmeyer³¹ compared the unit cell dimensions published by several authors, many of whom proposed several 'paracrystalline' forms to describe aberrations in the α and γ crystal forms unit cells. The authors instead found a continuous variation in the unit cell dimensions between α and γ nylon 6 rather than a sharp difference indicating much more complex behaviour than just a mixture of different crystal forms. It was also shown that X-ray patterns of samples containing both α and γ forms could not be simulated by a simple mixture of pure α and pure γ .

In our work on characterization of ¹⁵N-labelled nylon 6, spin lattice relaxation (*T*₁) measurements also

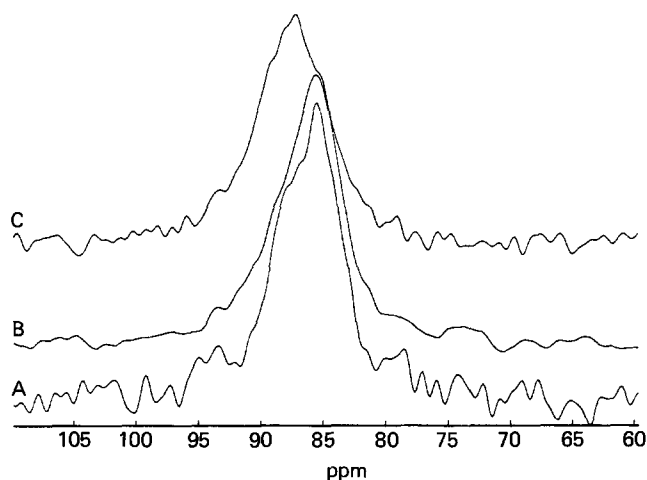


Figure 3 ¹⁵N CP/MAS n.m.r. spectra of annealed samples of: (A) nylon 7; (B) nylon 6-8; (C) nylon 6-9

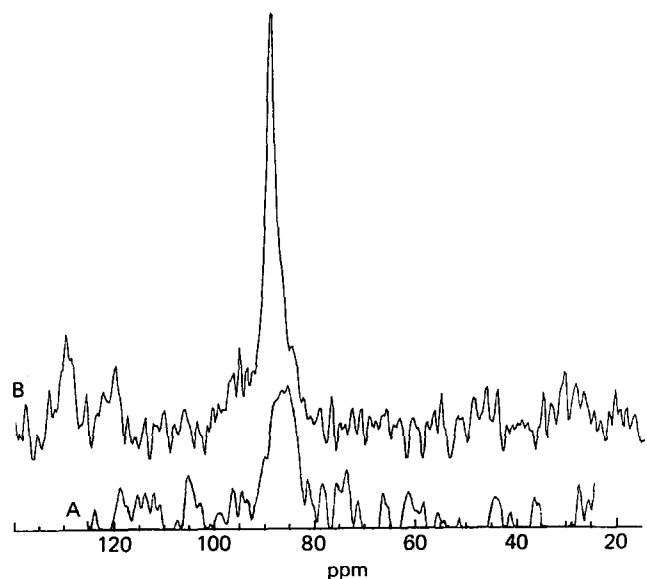


Figure 4 ¹⁵N CP/MAS n.m.r. spectra of (A) nylon 13-13 as-obtained and (B) after annealing for several hours

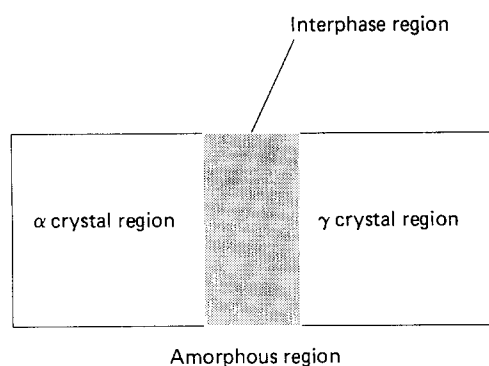


Figure 5 Schematic representation of proposed microenvironment of semicrystalline nylons

suggested the presence of rigid, non-crystalline regions with chemical shifts and relaxation times different from either the α or γ crystal forms^{13,14}. Based on these results and the data presented in *Tables 1* and *2*, it appears that ^{15}N CP/MAS n.m.r. is effective in probing material, and regions of the material, at the molecular level that can only be poorly characterized by X-ray. Examination of the spectrum in *Figure 6* of Zytel 330, a completely amorphous nylon, provides additional support. This sample shows no crystallinity by i.r. and X-ray analysis. However, a broad resonance is seen in the ^{15}N n.m.r. spectrum indicating a range of chemical environments in an overall amorphous polymer. This broad envelope of peaks is similar to that observed in *Figure 4* for nylon 13-13, and in ^{15}N -labelled nylon 6 and nylon 11 using pulse programs that allow selective observation of the more mobile amorphous domains^{14,15}. It should be mentioned, however, that this polymer contains both aromatic and aliphatic amide groups which possess different chemical shifts that contribute to the broadness of the peak observed. Thus, while Zytel 330 may not be a representative example of a completely amorphous nylon, the spectral data clearly show the potential for using solid state ^{15}N n.m.r. for the analysis of such materials.

The situation appears to correspond to that seen in the n.m.r. analysis of vinyl polymer stereochemistry. Racemic and meso units composing diads, triads and higher order sequences give individual peaks for many or all of the various combinations. Thus, even a non-stereoregular and non-crystalline vinyl polymer will show multiple peaks corresponding to specific repeat unit sequences. Nuclear magnetic resonance sees these sequences at the molecular or repeat unit level rather than at the overall or average compositional level. On the other hand, X-ray diffraction requires ordered arrays of molecules or polymer sequences that extend far beyond individual repeat units. Infra-red may see at both levels although the ability to resolve fragment differences is limited by the inherent peak width seen for polymer samples. Apparently, ^{15}N CP/MAS provides sufficient sensitivity and resolution to allow observation of segments smaller than those required for obtaining X-ray active α or γ crystalline domain. These may show up as peaks with the same chemical shifts as those of the larger crystals but with no detectable order by X-ray diffraction, or the conformations may vary over such a range that individual contributions are buried in the broad envelope of peaks observed for the amorphous regions.

These arguments are supported by a recent study³² of nylon 6 composites by ^{13}C CP/MAS n.m.r. The ^{13}C CP/MAS spectra of most samples showed the presence of two crystalline phases plus an amorphous component. While the carbonyl carbon had an identical chemical shift for all samples (an observation we have confirmed), aliphatic carbons directly attached to the amide group were shifted significantly in the two crystalline forms. In the α form, the CH_2 groups attached to the amide nitrogen and carbon were found at 42.8 and 36.8 ppm, respectively, while those of the γ form were seen at 39.9 and 33.9 ppm. This 3 ppm shift for each of these two methylenes was not observed for the other CH_2 groups which showed at most a 0.5 ppm difference between the two forms. These researchers attempted to correlate peak intensity with crystalline composition. Quantitation was hampered by overlapping peaks and differences in relaxation rates which make it difficult to subtract amorphous contributions to allow direct comparison of the α and γ components. Use of alternative pulse programs, however, can lead to easily separated ^{13}C peaks for the two crystal forms¹⁶. In addition, the ^{14}N quadrupole coupling was not detected in the ^{13}C spectra although (based on our experience) it should be present and lead to additional broadening of the peak for the CH_2 attached to nitrogen. Careful work by these authors³² led to consistent quantitation, although correlation with X-ray results was poor. The argument was advanced that the two techniques probe composition at different levels; i.e. solid state n.m.r. (at least of crystalline domains) looks at crystallites (0.5–1 nm) that are considerably smaller than those seen by X-ray (5–10 nm). Thus, the n.m.r. data gave consistently higher content values for a particular crystalline form than that calculated from X-ray diffraction data.

A further important conclusion from the ^{13}C CP/MAS study of nylon 6 was that both extrusion and the presence of additives and fillers gave increased γ content. In fact, our initial report on the ^{15}N CP/MAS of nylon 6 and its copolymers also showed that the presence of blocks of *p*-benzamide in nylon 6 copolymers induced formation of the normally less stable γ crystalline form¹¹. Our results fully support the findings available through solid state ^{13}C n.m.r. However, despite the fact that ^{15}N is a more difficult nucleus to examine by solid state n.m.r., the method is easy, straightforward and appears to be

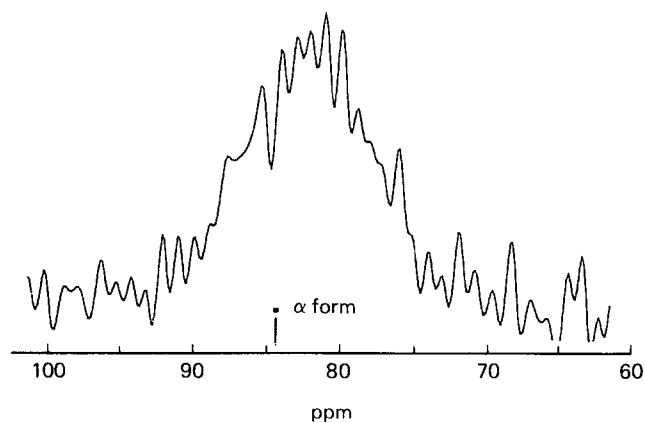


Figure 6 ^{15}N CP/MAS n.m.r. spectrum of Zytel 330 brand of amorphous nylon; the relative position of the α crystal form is shown for comparison

quantitative. For example, the broad α and γ resonances in the ¹³C alkyl region could only be resolved using peak deconvolution techniques while the ¹⁵N spectra reveal the two crystal forms explicitly. Use of the aliphatic carbon resonances for quantitative analysis is further complicated by the significant contribution of the amorphous fraction to the overlapping signals. Additional advantages include simpler spectra, greater peak separation and spectral width, direct observation of the atom of interest for hydrogen bonding and crystallinity differences, and (as will be shown below) a more sensitive chemical shift-conformation relationship for the range of dihedral angles involved.

Polypeptides

Natural and synthetic polypeptides are the only polyamides previously investigated¹⁹ by ¹⁵N CP/MAS n.m.r. Of the nylon species shown in Table 1, the polypeptides nylon 2 (polyglycine) and α -methyl nylon 2 (polyalanine) form two types of ordered structures. For nylon 2, the amide nitrogen chemical shift is upfield for the planar β sheet (74.0 ppm) and downfield for the twisted α helix (78.5 ppm), the order observed for similar conformations in the higher nylon homologues. Although the absolute values of the chemical shifts are different, the $\Delta\delta$ value of 4.5 ppm compares well with that of 4–5 ppm seen for the two main forms of nylon. The glycine-containing oligomers shown for comparison in Table 1 demonstrate the complexity of polymer crystallinity with increasing molecular weight. As the number of residues grows, more conformations are available, leading to more complex spectra. In most cases, however, their chemical shifts fall between those reported for α helix and β sheet polyglycine.

Polyalanine, however, shows the opposite effect. The twisted helix is now upfield (89.1 ppm) rather than downfield of the planar sheet (97.9 ppm). This must be due to a conformationally dependent substituent effect as described previously for ¹⁵N solution^{18–20} and solid state¹⁹ n.m.r. of several poly(amino acids). An alkyl substituent in the α position causes a downfield shift of ~9–12 ppm. In solution, of course, the peak position is an average of the chemical shifts of all allowed conformations. Nonetheless, this reverse shielding effect appears to be peculiar to α -substituted polypeptides. Complete understanding of the conformation dependency of ¹⁵N chemical shifts awaits appropriate studies with crystalline (for solid state behaviour) and conformationally rigid models (for solution analysis).

Linear nylon 3 [poly(β -alanine)] has been reported to exist only in the α crystal form^{25,27} and has a chemical shift (88.1 ppm) closer to that of the γ form seen in higher nylons. This result is inconsistent with the dihedral angles required by the helical structure in the absence of additional effects on the chemical shift. The next higher homologue (nylon 4), however, has a chemical shift of 85.2 ppm, within the range observed for higher nylon homologues. This inconsistency may be the result of secondary effects (similar to polypeptides) which become less important in higher nylon homologues. It is clear from the data in Table 1 that as the alkyl chain length between amide groups reaches three methylene units or beyond, secondary effects from adjacent amide units become less important and the ¹⁵N chemical shifts depend almost exclusively on amide conformation. The

¹³C CP/MAS chemical shift differences in peptides have been attributed to a combination of hydrogen bonding, conformational effects and helix formation³³. Interactions that affect the ¹⁵N chemical shift should be similarly more complex in short chain nylon analogues than in nylons with longer alkyl chains and for nylons with substituted methylene chains between the amide groups (as in the amorphous Zytel nylons).

Comparison of natural abundance spectra with ¹⁵N-enriched nylon samples

The CP/MAS spectrum of nylon 6 is shown in Figure 7B¹⁴. The spectrum shown is very similar to natural abundance ¹⁵N spectra of nylon 6. The main strong peak clearly overlaps a broader resonance at lower field. The overlapping peaks were fit with a composite lineshape (Figure 7A) and the individual components deconvoluted as shown. From the deconvoluted components, the upfield resonance is located at 84.2 ppm with a line width at half height of 2.4 ppm, consistent with the α crystal form^{11,12} of unlabelled nylon 6. The broader downfield resonance is centred at 87.2 ppm and possesses a line width at half height of 6.3 ppm. This resonance had not been observed in our previous work with polyamides at the ¹⁵N natural abundance level. This signal is assigned to the non-crystalline or 'amorphous' fraction of the nylon sample since its chemical shift appears midway between the α and γ resonances typically observed for nylon 6 and other nylons.

To conclusively identify the downfield resonance as

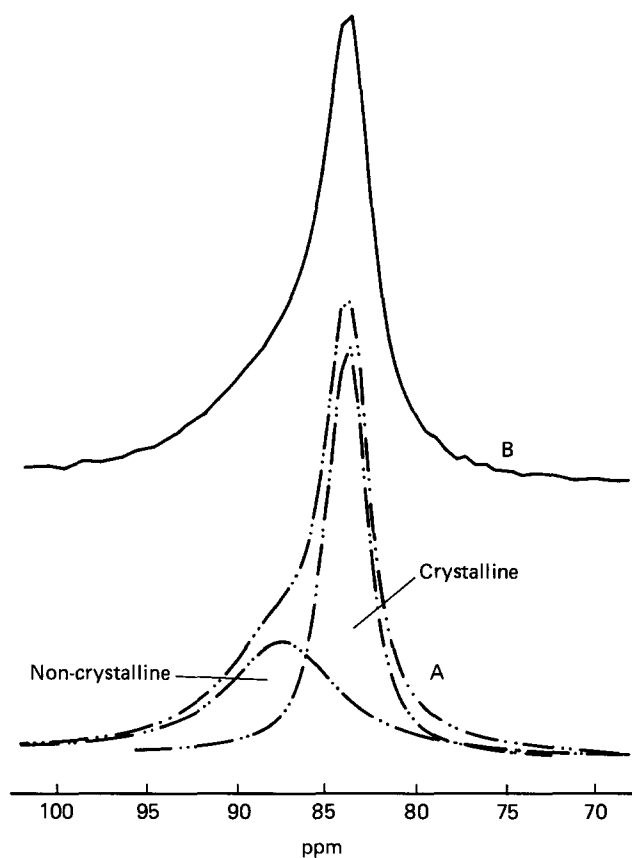


Figure 7 ¹⁵N CP/MAS spectrum (B, 18 000 free induction decays) of ¹⁵N-enriched nylon 6 showing α crystal form (large peak at ~84 ppm) and broader, overlapping region downfield (non-crystalline region); (A) shows a least squares fit of the ¹⁵N CP/MAS lineshape along with individual components

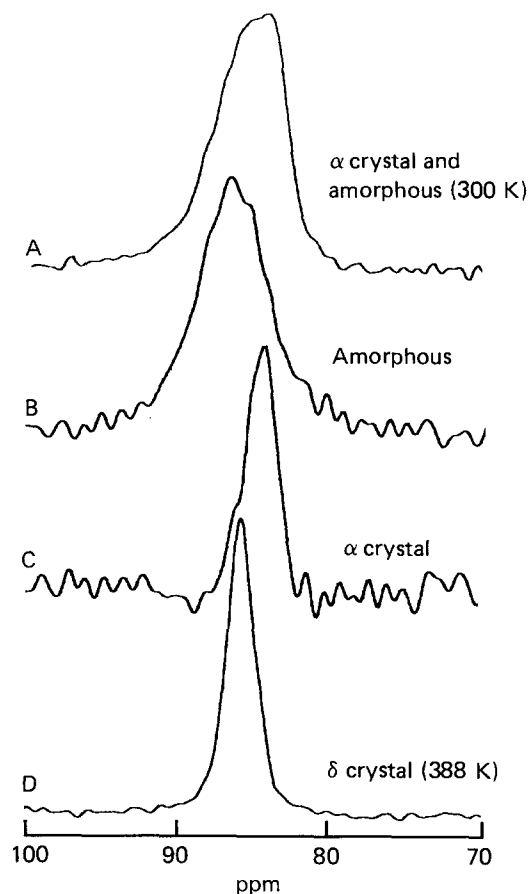


Figure 8 ¹⁵N n.m.r. spectra of isothermally annealed nylon 11: (A) CP/MAS spectrum obtained at 300 K; (B) was obtained by applying a 90° ¹⁵N pulse with proton decoupling to saturate the crystal resonance; (C) is the difference spectrum of (A) and (B) showing only the α crystal resonance at 84.2 ppm. The α crystal resonance disappears on heating above the 95°C (368 K) α-δ transition temperature to give the δ form seen in (D)¹⁵

that of the amorphous region, relaxation experiments were conducted to evaluate the mobility of each region by monitoring spin-lattice relaxation times (T_{1N})¹⁴. Using the method of Torchia³⁴, relaxation times T_{1N} were obtained at 300 K for resonances at 84.2 ppm (α crystal resonance) and 87.2 ppm (approximate centre of the amorphous resonance) for several samples. The crystalline component had a long T_{1N} , while the amorphous component of the same sample had two shorter T_{1N} s. The detection of two T_{1N} s indicates two types of amorphous regions, a bulk amorphous fraction with liquid-like mobility and a non-crystalline 'inter-phase' region with restricted motion (Figure 5). Similar phase morphology is observed in polyethylene where the crystalline component and the non-crystalline 'inter-phase' region are clearly differentiated by their T_{1C} relaxation times³⁵. The amorphous regions in all nylon samples we have examined have shorter ¹⁵N relaxation times than the crystalline regions, a fact consistent with ¹³C relaxation studies of these materials³².

The multiple peaks in Figure 2 for nylon 11 prompted the preparation of a ¹⁵N-enriched sample to evaluate different crystal forms possible for this polymer. Evidence of polymorphism in nylon 11 has been demonstrated by several workers and found to be dependent on the thermal history of the sample as well as the test temperature³⁶⁻⁴⁰. Thermal analysis and X-ray studies

point to two morphologies in samples isothermally annealed below the melting point; the α form which is stable at temperatures below 95°C^{37,41} and the δ form which exists at temperatures above 95°C⁴¹. The δ form is unstable at room temperature and reverts to the α form very rapidly on cooling. Samples quenched from the melt, on the other hand, have been shown to crystallize into the kinetically favoured but metastable δ' form^{42,43}.

The ¹⁵N CP/MAS spectrum of ¹⁵N-enriched nylon 11 annealed at 170°C is shown¹⁵ in Figure 8A. The most intense resonance is seen at 84.2 ppm (the α crystal form) with an equally intense and overlapping broad peak further downfield. The crystalline resonance was identical to that previously found for the α crystal form of nylon 6. The broad downfield resonance is also similar to the amorphous region seen in nylon 6. Using a 90° ¹⁵N pulse with decoupling (no CP), the MAS spectrum in trace B was obtained. The α crystal magnetization has been saturated, leaving only the fast relaxing amorphous component shown. Spectral subtraction of B from A gives the narrow α crystal resonance seen in trace C at 84.2 ppm. Trace D in Figure 8 shows the CP/MAS spectrum of the annealed sample obtained at 388 K (115°C), well above the reported α to δ transition temperature. Clearly the peak for the α crystal form has disappeared, leaving only a downfield resonance at 86.7 ppm. Also, the increased mobility of the amorphous regions at this temperature make CP so inefficient that peaks for the non-crystalline domains are not seen in trace D. Similar behaviour was seen for the ¹⁵N-labelled samples as well. Finally, the spectrum in trace D reverts rapidly to that in trace A again on cooling back to room temperature, confirming the reversibility of the transition.

Conformational effects on ¹⁵N chemical shift molecular modelling results

The origin of these chemical shift differences was originally unclear. It seemed reasonable at first that the chemical shift differences would be due to differences in hydrogen bonding in the crystalline and amorphous domains. In amorphous polyamides, however, i.r. studies indicate that nylon-like polyamides are completely hydrogen bonded making it improbable that the chemical shift change is due to some combination of 'free' and 'hydrogen bonded' amide units⁴⁴. In addition, X-ray studies show the hydrogen bond length in both the α and γ crystalline forms of nylon 6 to be identical to within 0.002 nm^{21,45}. Figure 1 suggests that the chemical shift difference may be due solely to conformationally dependent changes about the amide bond (at least for different crystal forms of nylons). This interpretation is supported by ¹⁵N n.m.r. solution spectra of N-substituted amides⁴⁶. E,Z isomers (about the planar amide C-N bond) can be observed as two distinct resonances separated by 1-3 ppm, and it seems reasonable that conformational changes about bonds attached to the amide group may also make an important contribution to chemical shift.

However, a simple relationship involving conformation is complicated by substituent effects. In ¹³C n.m.r. spectral results, replacement of hydrogens by other substituents, especially those γ to a carbon nucleus, exerts a strong effect on chemical shift (the 'γ gauche effect')^{47,48}. ¹³C CP/MAS n.m.r. has been shown to be sensitive to both secondary structure and substituents in peptides

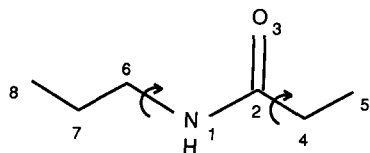


Figure 9 Model amide used in MO calculations. Dihedral angles: α form, 7, 6, 1, 2 = 1, 2, 4, 5 = 180°C; γ form, 7, 6, 4, 2 = 120° and 1,2,4,5 = 240°

and α -substituted nylons⁴⁵. The ¹³C CP/MAS spectra of α and γ nylon 6, however, show the carbonyl peaks to have identical chemical shifts³². The amide nitrogens are apparently more sensitive to conformation than are the carbonyl carbons. In more recent work involving the ¹⁵N CP/MAS spectra of peptides¹⁸, downfield shift effects were observed in peptides with a carbon substituent β to the nitrogen in addition to shifts related to α helix and β sheet conformations. A steric γ *gauche*-like effect for nitrogen may be responsible for this behaviour⁴⁹.

Further exploration of the potential of ¹⁵N n.m.r. to evaluate crystallinity and conformation requires additional n.m.r. analysis coupled with molecular modelling. SCF-MO and valence shell theory have both been used to predict shielding of nuclei as a function of 'effective nuclear charge' thus providing a method of correlating chemical shifts with local charge density^{50,51}. More importantly, perturbations in charge density have been related to conformational geometry and steric strain⁵⁰. Semi-empirical calculations have also been successful in reproducing experimental trends in magnetic shielding⁵².

Our initial efforts involving semi-empirical calculations on a model system were encouraging. Using an appropriate model amide, we calculated the heats of formation and electron distributions for the two conformations known to exist for the amide groups in the α and γ forms of nylons. One model (*Figure 9*) consists of a central amide with two n-propyl fragments attached to the carbonyl and nitrogen atoms. The α form calculation was for an extended planar zig-zag of the methylene chains with the amide group lying in this plane. All bond lengths, bond angles and dihedral angles for the α model were fully optimized. The γ form model had the amide plane rotated 60° from the two coplanar methylene chains attached to either side of the amide^{21,22}. The amide plane dihedral angle with respect to the attached methylenes was fixed throughout the calculation and all other parameters were allowed to optimize.

The atom electron density is calculated according to⁵³:

$$q_{\text{atom}} = \sum_1^i n c_i^2 \quad (1)$$

where n is the number of electrons in an occupied orbital (two for unperturbed ground state) and c_i is the i th coefficient of each secular equation describing a localized orbital. The net charge on each atom is defined by:

$$q_{\text{net}} = q_{\text{val}} - q_{\text{atom}} \quad (2)$$

where q_{val} is the normal atom valence. *Table 3* lists the calculated charges for the amide nitrogens, carbons and oxygens in this model.

The α form nitrogen has higher electron density as indicated by the relative charge (−0.393 *versus* −0.378) than that of the γ conformation, consistent with a more

shielded, upfield chemical shift value for this nitrogen. Similarly, the oxygen of the α form was more electron poor than that of the γ form but the difference was surprisingly small. The carbonyl and C_α carbons showed little difference in charge which correlates well (for the former) with the observation of nylon 6 in the two main crystalline forms by ¹³C CP/MAS n.m.r.³².

Table 3 shows a large build-up of charge on C_N which should result in an upfield shift in the ¹³C n.m.r. As discussed earlier, this prediction was verified by Weeding and co-workers in their study of nylon 6 composites with ¹³C CP/MAS n.m.r.³². The C_N resonance of the γ form was shifted upfield by almost 3 ppm from the α crystal form. Nevertheless, the build-up of charge on C_N was unexpected. Redistribution of charge density from the nitrogen to oxygen via conjugated π orbitals in the amide group seems more reasonable while movement of charge from the nitrogen to C_N via a σ bond seems less likely. Another possible explanation is that protons on C_N are somehow influencing the charge distribution by through-space interaction with the amide group. This hypothesis was supported by ¹H and ¹³C n.m.r. characterization of cyclic glycol peptides where the C–H coupling constant behaviour, which is dependent on conformation, was rationalized as an interaction of the C–H bond with the nitrogen p_z orbital⁵⁴.

To test this hypothesis, we modelled several small molecules using AMPAC and varied the torsion angle of substituents with the plane of the amide group. Two possible interactions were contemplated: the interaction of protons on the N -alkyl substituent with the nitrogen atom; and the interaction of protons on C_α and C_β with the amide π orbital. *Figure 10* shows a plot of nitrogen charge *versus* the torsion angle for the methyl group of

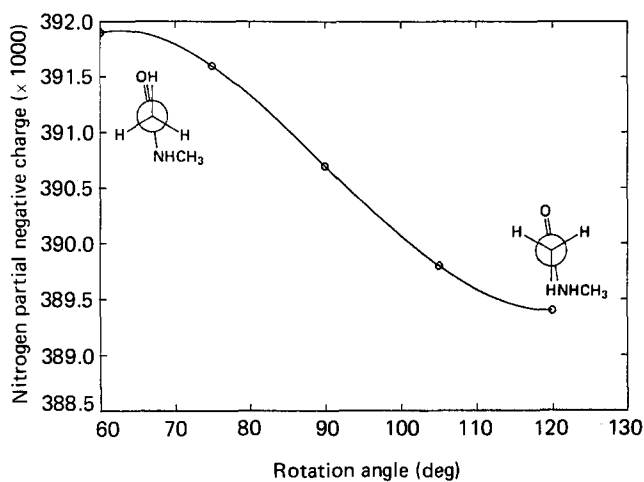


Figure 10 Plot of calculated partial nitrogen charge as a function of α methyl rotation for N -methyl acetamide

Table 3 Calculated partial charges for planar and twisted conformations of N -n-propyl propionamide

Atom	Planar form (α)	Twisted form (γ)	Δq ($\alpha - \gamma$)
N	−0.393	−0.378	−0.015
O	−0.369	−0.372	0.003
C (carbonyl)	0.298	0.298	0.000
C_α	−0.178	−0.177	−0.001
C_N	−0.019	−0.032	0.013

Table 4 AM1 calculation results for amide model compounds

Molecule	Charge on N	Chemical shift	
		CH ₃ NO ₂ (0 ppm ^a)	DMF (0 ppm)
Formamide	-0.448	-269.1 ^b	7.6
<i>N</i> -methyl formamide	-0.4023	-270.1 ^b	6.6
Acetamide	-0.440	-271.0 ^b	5.7
<i>N</i> -methyl acetamide	-0.391	-273.7 ^b	3.0
<i>N</i> -ethyl acetamide	-0.390	-254.8 ^b	21.9
<i>N</i> - <i>n</i> -propyl acetamide	-0.3807	-260.4 ^c	16.3
<i>N</i> - <i>i</i> -propyl acetamide	-0.3823	-244.1 ^c	32.6
<i>N</i> - <i>t</i> -butyl acetamide	-0.3803	-241.8 ^c	34.9
<i>N</i> -methyl propionamide	-0.3959	-276.5 ^b	0.2
<i>N</i> -methyl isobutanamide	-0.3890	-278.4 ^b	-1.7
<i>N,N</i> -dimethyl formamide	-0.3527	-276.7 ^d	0.0
<i>N,N</i> -diethyl formamide	-0.3473	-250.2 ^d	26.5
<i>N,N</i> -dimethyl acetamide	-0.3457	-281.0 ^d	-4.3
<i>N,N</i> -diethyl acetamide	-0.3404	-249.6 ^d	27.1

^aChemical shifts and experimental conditions reported in ref. 55^bNeat liquid^c60% in CHCl₃^dChromium acetylacetonate (0.08 M) added to neat liquid

N-methyl acetamide. A maximum is seen for the form in which the C_α protons are *gauche* to nitrogen (60° rotation angle). This agrees qualitatively with the n.m.r. data in that increased electron density results in nuclear shielding and corresponding upfield shifts. Similar results are obtained for acetamide and *N*-ethyl acetamide. For the latter, however, an even more drastic decrease in electron density is seen consistent with a downfield shift on going from the planar α form to the twisted γ form.

The success of these initial calculations prompted us to extend this series. Additional model systems were generated and their atom partial charges calculated to test whether protons γ to the amide nitrogen could alter the nitrogen electron density. Table 4 shows the optimized results for the AMPAC models of calculated partial charge on the nitrogen atom. The ¹⁵N solution n.m.r. chemical shifts are reported for comparison⁵⁵. For convenience, arbitrary chemical shifts are listed relative to dimethyl formamide (DMF = 0 ppm) to allow most of the chemical shifts to be displayed as positive values.

Ideally, as partial negative charge increases or decreases on the nitrogen, there should be a corresponding upfield or downfield shift, respectively, in the ¹⁵N chemical shift. Since the effects of solvents, hydrogen bonding and sample concentration are ignored in gas phase AMPAC calculations, the AMPAC partial charges cannot predict chemical shifts quantitatively. For example, in comparing the primary amides with those having one *N*-methyl substituent, AMPAC predicts a large downfield shift upon alkylation of the nitrogen. The reported chemical shifts show almost no change. This suggests that hydrogen bonding and other intermolecular interactions exert major influence on chemical shifts in solution. In the higher alkyl homologues, especially the *N*-alkyl acetamides where substituents R on the nitrogen are varied, a reasonably consistent trend is observed. AMPAC predicts an increase in nitrogen charge as R is varied from 3° < 2° < 1° < methyl. The chemical shifts reported for these amides follow approximately this order with *t*-butyl acetamide having the largest downfield shift and lowest calculated nitrogen charge. AMPAC predicts little if any difference in nitrogen atom charge

on increasing the chain length of the carbonyl substituent. The n.m.r. data, however, show an upfield trend for the series of *N*-methyl amides. While AMPAC appears to fail in its predictions here, it should be noted that the chemical shift range ($\Delta\delta$) for this series is only ~5 ppm, well within the range where experimental variables could account for discrepancies. The *N*-alkyl acetamides, on the other hand, show a total $\Delta\delta$ of almost 30 ppm which can only be related to a substituent effect.

In evaluating these model systems, it is important to remember they represent gas phase behaviour and ignore dipolar interactions, hydrogen bonding and other effects present in both the solid state and in solution. It must also be remembered that the solution chemical shifts given in Table 4 represent conformationally averaged values while the calculated values are for only a single conformation. Semi-empirical MO methods have been remarkably successful in the past in predicting properties for which they were not parameterized⁵⁶. As previously mentioned, quantum chemical calculations have shown the ¹³C CP/MAS chemical shift of peptides to be affected by both hydrogen bonding and conformation³³. The hydrogen bond contribution to ¹³C chemical shifts is reported⁴¹ to be dominant for N–O bond lengths <0.26 nm. For both α and γ nylons, the N–O bond length⁴⁵ is >0.28 nm. At these distances, hydrogen bond strength drops off rapidly leaving conformational interactions to dominate the chemical shift in ¹³C CP/MAS n.m.r. ¹⁵N CP/MAS chemical shifts appear to be similarly influenced.

Although hydrogen bonding is not accounted for in these quantum chemical models, the electronic structures simulate α and γ nylon chemical shift trends remarkably well. If the total nitrogen shielding σ for each of the conformations is represented by equations (3) and (4):

$$\sigma_{\alpha} = \sigma_{E\alpha} + \sigma_{H\alpha} \quad (3)$$

$$\sigma_{\gamma} = \sigma_{E\gamma} + \sigma_{H\gamma} \quad (4)$$

where σ_E is the sum of local electronic contributions and σ_H is the shielding induced by hydrogen bond perturbation of the system, the terms σ_H may be eliminated provided $\sigma_{H\alpha} = \sigma_{H\gamma}$. The assumption of $\sigma_{H\alpha} = \sigma_{H\gamma}$ is probably valid for nylons since the hydrogen bond lengths and orientations are nearly equivalent for the α and γ crystal forms⁴⁵. An alternative explanation may be that the α and γ structures lie in the domain of long hydrogen bond lengths where conformation, not hydrogen bonding, exerts the major influence on the chemical shift⁴⁵. In this case, σ_H in equations (3) and (4) can be effectively ignored. Either case implies that the differences in the total shielding, and ultimately the chemical shifts, are due to local electronic contributions principally affected by conformation.

An additional observation should be made about Figure 10. AMPAC calculations not only predict a change in nitrogen electron density with amide group rotation, but also predict that the α and γ conformations are the most and least shielded, respectively. This suggests that amide groups in other conformations will have ¹⁵N chemical shifts between 84 ppm and 89 ppm. An examination of the chemical shifts of the most intense peaks in Table 1 shows this to be the case with the exception of some peptide oligomers and polymers. This strongly supports our assertion that ¹⁵N chemical shifts in polyamides are sensitive to amide conformation and,

coupled with molecular modelling, may be able to predict the local conformation of amide groups in the solid state. It also suggests that other nylon crystal forms, as well as non-crystalline or amorphous regions, will have chemical shifts that lie between those of the α and γ peaks in the n.m.r. spectrum. In fact, results from ¹⁵N-enriched nylon 6 and nylon 11 have confirmed the presence of amorphous components and two additional crystalline forms (δ and δ'), all with chemical shifts between those of the α and γ crystal forms^{14,15}.

CONCLUSIONS

Characteristic ¹⁵N n.m.r. resonances are reported for a series of aliphatic polyamides and correlated with their predominant crystal forms, generally α and γ forms. We have further observed and catalogued peaks which correspond to amorphous regions and/or amide interphase domains which are difficult to observe or characterize by other techniques. Conclusive assignment of these intermediate resonances to the amorphous regions of natural abundance samples was hampered by poor signal-to-noise of the spectra as well as by lack of corroborating n.m.r. evidence (e.g. T_{1N} relaxation experiments). In order to address this problem, we prepared ¹⁵N-labelled analogues of two important commercial polyamides: polycaproyamide (nylon 6, 20% ¹⁵N enrichment) and polyundecanamide (nylon 11, 99% ¹⁵N enrichment). CP/MAS experiments on these samples confirmed our initial observations of characteristic chemical shifts for both crystalline and amorphous regions. The observed chemical shifts and relaxation data for the ¹⁵N-enriched samples support assignments for natural abundance samples. Chemical shift differences appear to be due to conformational as well as substituent effects, perhaps in a manner similar to the γ *gauche* effect previously observed in ¹³C n.m.r. The conformational relationship is supported qualitatively by semi-empirical MO calculation results which correlate well with the experimental data.

We conclude that natural abundance ¹⁵N CP/MAS n.m.r. analysis of nitrogen-containing polymers is not only feasible but is a sensitive measure of composition, conformation, crystalline form and amorphous content.

ACKNOWLEDGEMENTS

We gratefully acknowledge a Department of Defense instrumentation grant, through the Office of Naval Research, with which we purchased our Bruker MSL-200 spectrometer. This research was supported in part by a grant from the Office of Naval Research. We thank the following for providing samples and additional characterization data: J. P. Autran and R. S. Porter (University of Massachusetts), K. H. Gardner and R. A. Vaidya (DuPont) and R. Bacskai (Chevron Research). We also thank Dr Andrew Holder, of Professor Dewar's group at the University of Texas at Austin, for helpful discussions of our molecular modelling efforts.

REFERENCES

- 1 Ferry, J. D. 'Viscoelastic Properties of Polymers', 3rd Edn, John Wiley and Sons, New York, 1980
- 2 Koenig, J. L., Ipecki, M. and Lando, J. B. *J. Macromol. Sci. Phys.* 1972, **B6** (4), 713

- 3 Heuvel, H. M. and Huisman, R. *J. Appl. Polym. Sci.* 1981, **26**, 713
- 4 Fyfe, C. A. 'Solid State NMR for Chemists', CFC Press, Guelph, 1983
- 5 Spiess, H. W. in 'Advances in Polymer Science 66', Springer-Verlag, Berlin, 1985
- 6 Komoroski, R. A. (Ed.) 'High Resolution NMR Spectroscopy of Synthetic Polymers in Bulk', VCH Publishers, Deerfield Beach, 1986
- 7 Moore, D. R. and Mathias, L. J. *J. Appl. Polym. Sci.* 1986, **32**, 6299
- 8 Mathias, L. J., Moore, D. R. and Smith, C. A. *J. Polym. Sci., Polym. Chem. Edn* 1987, **25**, 2699
- 9 Sikes, A. M. and Mathias, L. J. *Polym. Bull.* 1987, **18**, 397
- 10 Moore, D. R. and Mathias, L. J. *Polym. Composites* 1988, **9**, 144
- 11 Powell, D. G., Sikes, A. M. and Mathias, L. J. *Macromolecules* 1988, **21**, 1533
- 12 Mathias, L. J., Powell, D. G. and Sikes, A. M. *Polym. Commun.* 1988, **29**, 192
- 13 Powell, D. G. and Mathias, L. J. *Macromolecules* 1989, **22**, 3812
- 14 Powell, D. G. and Mathias, L. J. *J. Am. Chem. Soc.* 1990, **112**, 669
- 15 Mathias, L. J., Powell, D. G., Autran, J.-P. and Porter, R. S. *Macromolecules* 1990, **23**, 963
- 16 Hatfield, G. R., Glans, J. H. and Hammond, W. B. *Macromolecules* 1990, **23**, 1654
- 17 Dewar, M. J. S., Zoebisch, E. G., Healy, E. F. and Stewart, J. P. *J. Am. Chem. Soc.* 1985, **107**, 3902
- 18 Kricheldorf, H. R. *Pure Appl. Chem.* 1982, **54**, 467
- 19 Forster, H. G., Muller, D. and Kricheldorf, H. R. *Int. J. Biol. Macromol.* 1983, **5**, 101
- 20 Shoji, A., Ozaki, T., Fujito, T., Deguchi, K. and Ando, I. *Macromolecules* 1987, **20**, 2441
- 21 Arimoto, H., Ishibashi, M. and Hirai, M. *J. Polym. Sci., Polym. Chem. Edn* 1965, **3**, 317
- 22 Gianchadani, J., Spruiell, J. E. and Clark, E. S. *J. Appl. Polym. Sci.* 1982, **27**, 3527
- 23 Slichter, W. P. *J. Polym. Sci.* 1959, **36**, 259
- 24 Kinoshita, Y. *Makromol. Chem.* 1959, **33**, 1
- 25 Masamoto, J., Sasaguri, K., Ohizumi, C. and Kobayashi, H. *J. Polym. Sci. A2* 1970, **8**, 1703
- 26 Fredericks, R. J., Dayne, T. H. and Sprague, R. S. *J. Polym. Sci. A2* 1966, **4**, 913
- 27 Murthy, N. S., Szollosi, A. B. and Sibilia, J. P. *J. Polym. Sci., Polym. Phys. Edn* 1985, **23**, 2369
- 28 Miyake, A. *J. Polym. Sci.* 1960, **44**, 223
- 29 Miller, K. L. in 'Polymer Handbook' (Eds J. Brandrup and E. H. Immergut), 2nd Edn, John Wiley and Sons, New York, 1975, Ch. 3, p. 26
- 30 Statton, W. O. *J. Polym. Sci., Polym. Lett. Edn* 1967, **18**, 33
- 31 Parker, J. P. and Lindenmeyer, P. H. *J. Appl. Polym. Sci.* 1977, **21**, 821
- 32 Weeding, T. L., Veeman, W. S., Gaur, H. A. and Huysmans, W. G. B. *Macromolecules* 1988, **21**, 2028
- 33 Ando, S., Ando, I., Shoji, A. and Ozaki, T. *J. Am. Chem. Soc.* 1988, **110**, 3380
- 34 Torchia, D. A. *J. Magn. Reson.* 1978, **30**, 613
- 35 Kitamura, R., Fumitaka, H. and Murayama, K. *Macromolecules* 1986, **19**, 1943
- 36 Genas, M. *Angew. Chem.* 1962, **74**, 535
- 37 Slichter, W. P. *J. Polym. Sci.* 1959, **36**, 259
- 38 Little, K. *Br. J. Appl. Phys.* 1959, **10**, 225
- 39 Dosiere, M. and Point, J. J. *J. Polym. Sci., Polym. Phys. Edn* 1983, **21**, 625
- 40 Kawaguchi, K., Ikawa, T. and Fujiwara, Y. *J. Macromol. Sci.* 1981, **B20**, 1
- 41 Newman, B. A., Sham, T. P. and Pae, K. D. *J. Appl. Phys.* 1977, **48**, 4092
- 42 Schmidt, G. F. and Stuart, H. Z. *Z. Naturforsch.* 1958, **13**, 222
- 43 Chen, P. K., Newman, B. A. and Scheinbeim, J. I. *J. Mater. Sci.* 1985, **20**, 1753
- 44 Skrovanek, D. J., Howe, S. E., Painter, P. C. and Coleman, M. M. *Macromolecules* 1985, **18**, 1676
- 45 Tashiro, K. and Tadokoro, H. *Macromolecules* 1981, **14**, 781
- 46 Dorie, J., Grouesnard, J. P., Mechin, B., Naulet, N. and Martin, G. *J. Org. Magn. Reson.* 1980, **13**, 126
- 47 Whitesell, J. K. and Minton, M. A. *J. Am. Chem. Soc.* 1987, **109**, 225
- 48 Whitesell, J. K., LaCour, T., Lovell, R. L., Pojman, J., Ryan, P. and Yamada-Yosaka, A. *J. Am. Chem. Soc.* 1988, **110**, 991

- 49 Kricheldorf, H. R. and Muller, D. *Macromolecules* 1983, **16**, 615
50 Grant, D. M. and Cheney, B. V. *J. Am. Chem. Soc.* 1967, **89**, 5315
51 Cheney, B. V. and Grant, D. M. *J. Am. Chem. Soc.* 1967, **89**, 5319
52 Ditchfield, R., Miller, D. and Pople, J. *J. Chem. Phys.* 1971, **54**, 4168
53 Isaacs, N. 'Physical Organic Chemistry', John Wiley and Sons, New York, 1987
54 Egli, H. and von Philipsborn, W. *Helv. Chem. Acta* 1981, **64**, 976
55 Martin, G., Martin, M. and Gouesnard, J.-P. '¹⁵N-NMR Spectroscopy', Springer-Verlag, Berlin, 1981, pp. 135-137
56 Dewar, M. J. S., Landman, D., Suck, S. H. and Weiner, P. K. *J. Am. Chem. Soc.* 1977, **99**, 3951